ChemPubSoc Europe

DOI: 10.1002/open.201500154

Open Access ChemistryOPEN Full Papers

Electronic Property Modulation of One-Dimensional Extended Graphdiyne Nanowires from a First-Principle Crystal Orbital View

Ying Zhu,[a] Hongcun Bai,[b] and Yuanhe Huang*[a]

Graphdiyne and derivatives with delocalized π-electron systems are of particular interest owing to their structural, electronic, and transport properties, which are important for potential applications in next-generation electronics. Inspired by recently obtained extended graphdiyne nanowires, explorations of the modulation of the band gap and carrier mobility of this new species are still needed before application in device fabrication. To provide a deeper understanding of these issues, herein we present theoretical studies of one-dimensional extended graphdiyne nanowires using first-principle calculations. Modulation of the electronic properties of the extended graphdiyne nanowire was investigated systemically by considering several chemical and physical factors, including electric field, chemical functionalization, and carbo-merization. The band gap was observed to increase upon application of an electric field parallel to the plane of the synthesized graphdiyne nanowire in a non-periodic direction. Although chemical functionalization and carbo-merization caused the band gaps to decrease, the semiconducting property of the nanowires was preserved. Band gap engineering of the extended graphdiyne nanowires was explored regarding the field strength and the number of –C≡C– units in the carbon chain fragments. The charge carrier mobility of chemically functionalized and carbo-merized extended graphdiyne nanowires was also calculated to provide a comparison with pristine nanowire. Moreover, crystal orbital analysis was performed in order to discern the electronic and charge transport properties of the extended graphdiyne nanowires modified by the aforementioned chemical and physical factors.

Introduction

In the past two decades, carbon nanostructures and materials such as fullerenes, carbon nanotubes (CNTs), and graphene have been used in many practical devices. Furthermore, these materials possess the potential for further applications in state-of-the-art materials science and nano-scaled electronics.[1–5] This can be attributed to the abundant hybridization states (sp, sp^2, sp^3) of carbon, which affords the capacity to form complicated networks. This is a fundamental principle of organic chemistry and is also the basis for the existence of life. In recent years, graphene and its derivatives have elicited considerable attention due to their unique structures and properties.[6–10] Moreover, carbon chains composed of –C≡C– units are predicted to exhibit highly beneficial mechanical, charge-transport, electronic, and nonlinear optical properties.[11–16] Long atomic carbon chains have also been observed either inside multi-walled carbon nanotubes or as a linker between two nano-scaled graphene fragments.[17–22] State-of-the-art organic synthesis has also allowed the expansion of an original molecular system through the insertion of –C≡C– units into the chemical bonds of a molecule.[23] These structures are defined as the "carbo-mers" of the original molecules.[23] Using this strategy, various fascinating molecules such as carbo-merized benzene and carbo-merized cubane[24–28] have been synthesized. In 2010, Li et al. fabricated large-area ordered graphdiyne films in high-yield for the first time.[29] Structurally, graphdiyne can be considered the structure of one-third of the C–C bonds in graphene inserted with two –C≡C– units. This newly obtained species of carbon networks with delocalized π-electron systems are of particular interest owing to their electronic, optical, and geometric characteristics.[30–34] The highly conjugated, carbon-rich graphdiyne and its analogues featuring tunable structural and optoelectronic properties have also been recognized as promising candidates for use in next-generation electronic and optoelectronic devices.[35–39] Graphdiyne nanowalls, as well as one-dimensional (1D) nanoribbons and nanotubes derived from two-dimensional (2D) graphdiyne have also been obtained experimentally.[40–42]

Most recently the 1D extended graphdiyne nanowire shown in Scheme 1 was reported by Cirera et al. using surface-assisted covalent synthesis,[43] which is the basis of this work. Conjugat-

[a] Y. Zhu, Prof. Y. Huang
College of Chemistry, Beijing Normal University
No. 19, Xinjiekouwai Street, Beijing 100875 (P.R. China)
E-mail: yuanhe@bnu.edu.cn

[b] Dr. H. Bai
Key Laboratory of Energy Sources and Chemical Engineering
Ningxia University
No. 539, Helanshan Road, Yinchuan, Ningxia 750021 (P.R. China)

Supporting information for this article is available on the WWW under http://dx.doi.org/10.1002/open.201500154.

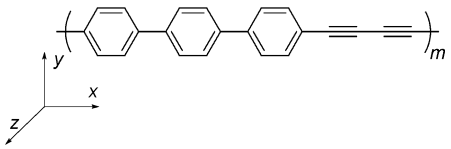

Scheme 1. The synthesized 1 D extended graphdiyne nanowire.

ed chains with structures similar to that of the extended graphdiyne wire, functionalized with chemical substituents, were also obtained.[44,45] 1 D materials have attracted substantial attention in recent years due to their unique properties that differ markedly from those of 2 D and three-dimensional (3 D) structures.[46,47] Furthermore, 1 D nanostructures are essential because they are the building blocks of various 2 D slabs and 3 D solid-state structures. Therefore, such extended graphdiyne nanowires would be new and interesting carbon materials that are widely anticipated for future applications.

Using first-principle calculations, the 1 D nanostructure of graphdiyne was shown to be a 1 D semiconductor with a simple band structure and a desirably small band gap.[43] Nevertheless, modulation of the electronic band gap is essential for future applications of semiconductors. This is because the application of such new organic polymer-based semiconducting optoelectronics requires a much more thorough understanding of the nature of the electronic structure and charge-transport properties.[48,49] Various physical or chemical methods have been suggested[50–61] in order to realize this goal. For instance, the electronic structures of CNTs can be readily manipulated under electric fields. In some cases, a semiconductor/metal transition can even be achieved.[50,51] The effects of substituent groups on the band gap and charge carrier mobility of graphene nanoribbons (GNRs) has been explored by Wang and Ge.[52] Previous studies have acknowledged that the addition of $-C\equiv C-$ units into the chemical bonds not only expands the skeleton, but also opens a band gap of original graphene.[53,54] Therefore, carbo-merization would be a good strategy for modifying the functional properties of low-dimensional nanostructures.

The aim of this work is to determine how an electric field, chemical functionalization at the benzene edges, and carbomerization affect the electronic properties of the recently obtained 1 D extended graphdiyne nanowires. Herein we report theoretical studies of the 1 D extended graphdiyne nanowires using a first-principle self-consistent field crystal orbital (SCF-CO) method under the framework of density functional theory (DFT). We anticipate that these studies will promote our understanding of this state-of-the-art research subject.

Results and Discussion

Band gaps under electric fields

The electronic structures of the extended graphdiyne nanowires are calculated under electric fields with varying strengths in the range of 0.25–3.0 V Å^{-1} (the step size is 0.25 V Å^{-1}). The field is applied in a direction perpendicular to the wire axis and parallel to the plane (i.e., along the *y*-axis direction of the coordinate system; Scheme 1) of the extended graphdiyne nanowire.

The obtained electronic band structures are shown in Figure 1. We first examined the case without an applied external field. Based on the band structure shown in Figure 1 a, it is clear that the extended graphdiyne nanowire has a direct band gap (E_g) between the top of the highest occupied band (HOB) and the bottom of the lowest unoccupied band (LUB). Therefore, the nanowire can be classified as a semiconductor with a band gap of 1.762 eV using the PBE method (2.605 eV with HSE06). This is similar to the 1.60 eV value obtained from previous DFT calculations by Cirera et al.[43] We then examined the results after the application of an external electric field. It was observed (Figure 1) that the energy band levels are changed somewhat. However, the shapes of the bands are well preserved when an electric field is applied. A band gap is always present whenever an external field with varying strengths is applied. These results suggest that the applied electric field cannot alter the semiconducting property of the 1 D nanowire. Moreover, the change of the band gaps from 1.762 to 2.000 eV with PBE (or 2.605 to 2.839 eV with HSE06,

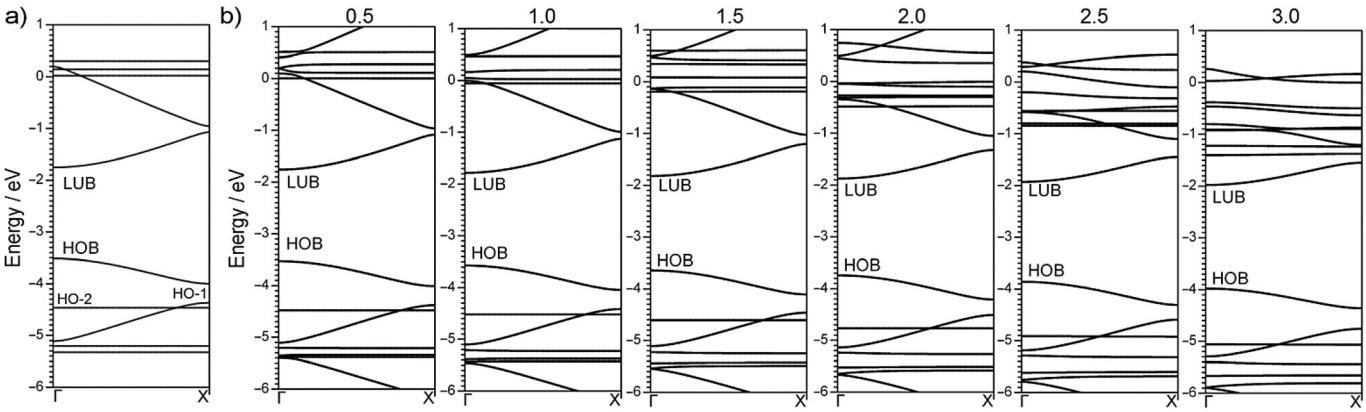

Figure 1. Electronic band structures of extended graphdiyne nanowire under a) zero field and b) external fields with various strengths (in V Å^{-1}). The band gaps are 1.762, 1.769, 1.788, 1.822, 1.868, 1.928, and 2.000 eV under the external fields of 0.0, 0.5, 1.0, 1.5, 2.0, 2.5 and 3.0 V Å^{-1}, respectively.

see Table S1, Supporting Information) is not substantial. The band gaps also exhibit an increasing trend when the field strength is enhanced to 3.0 V Å^{-1}. However, according to previous DFT calculations, the band gaps of CNTs, GNRs, and graphdiyne strips can decrease and sometimes even vanish with an increasing field.[50,51,60,61] Thus, the specific response of a 1D extended graphdiyne wire to an electric field is antithetical to the behavioral trends observed in CNTs, GNRs, and graphdiyne nano-scaled strips. This is an interesting phenomenon. Because the band gaps become even larger with the application of an electric field, we may expect that the applied electrical field would not cause a semiconductor/metal transition in the 1D extended graphdiyne nanowires. This fact is essential to the construction of electronic nanodevices, as the semiconducting property of the 1D extended graphdiyne nanowire can be easily maintained even with an electric field.

The band structures in Figure 1 show that the energy levels at the bottoms of the LUBs are very close, with a range of −1.468–1.535 eV under varying field strengths. The energy levels for the tops of the HOBs range from −3.578 to −4.001 eV, which means that there is a wider range for the HOB energy levels than the LUB energy values (0.423 vs. 0.067 eV). Thus, the band gap differences that are induced by the electric field are mainly attributed to variations in the HOB in the extended graphdiyne nanowire. To gain more insight into the band gap variations under electric fields, the highest occupied crystal orbital (HOCO) and the lowest unoccupied crystal orbital (LUCO) of the 1D extended graphdiyne nanowire are shown in Figure 2. The crystal orbital delocalizes in a longitudinal direction within the carbon chain fragment for both the HO and LU orbitals. However, the situation is rather different for the phenylene fragment. The crystal orbital spreads vertically in a longitudinal direction in the HOCO and along the longitudinal direction in the LUCO. The HOCO of the extended graphdiyne nanowire is more drastically influenced by an applied field because it is oriented parallel to the field. This influence is less significant in the LUCO because the crystal orbital distribution is always vertical to the applied electric field. This explains why the energy levels of the HOB for extended graphdiyne nanowires are more sensitive to electric fields than the energy level of the LUB.

Because the prepared graphdiyne nanowire can be treated as a junction of the polyphenylene and atomic carbon chain, calculations of the 1D polyphenylene and carbon chain under an electric field were also performed using the same computational methods in order to compare the obtained values. As shown in Figure 3, the band gaps of the isolated 1D polyphenylene and the carbon chain with bond length alternation (BLA) are 2.111 and 0.228 eV (close to 0.34 eV by previous DFT-GGA calculations[62]), respectively, in the absence of an electric field. The application of an increasing electric field causes the band gaps of polyphenylene to also increase, which was similarly observed in the extended graphdiyne wire. Figure 3 also shows that the band gaps vary more rapidly for polyphenylene than 1D extended graphdiyne wire.

This implies that the band gaps of polyphenylene are more flexible if an electric field is applied. However, the band gaps of the atomic carbon chain under the electric fields are nearly unchanged (< 0.01 eV compared with the absence of an applied field). This difference can be attributed to the distinct HOCO and LUCO shown in Figure 2. The HOCO and LUCO are both oriented along the direction of the wire axis for the carbon chain, whereas the HOCO and LUCO for polyphenylene are oriented in a vertical and parallel fashion, respectively. Studies of the extended graphdiyne wire show that the orbital

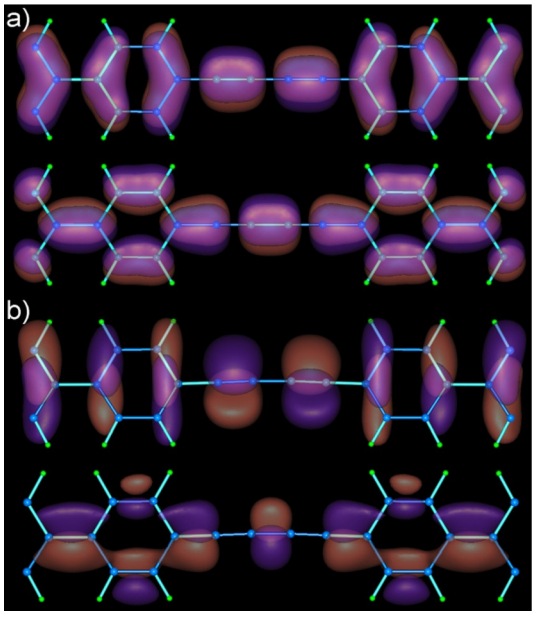

Figure 2. HOCO (upper) and LUCO (lower) of the 1D extended graphdiyne nanowire under a) zero field and b) electric field of 1.0 V Å^{-1}.

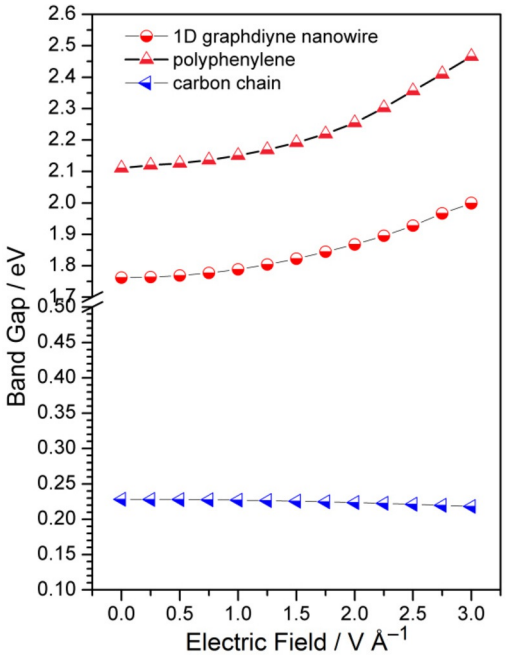

Figure 3. Relationship of band gap and field strength for the 1D extended graphdiyne nanowire.

distributions fall between the isolated polyphenylene and atomic carbon chain. Therefore, the effects of band gap modulation with an electrical field for polyphenylene are greater than both the extended graphdiyne nanowires and the carbon chain.

To gain more quantitative information about the relationship between the band gaps and the field strengths, the band gaps E_g (in eV) of the extended graphdiyne wire under an applied electric field strength E (in V Å^{-1}) are fit to the equation: $E_g = 0.024E^2 + 1.760$ using the PBE method ($E_g = 0.023E^2 + 2.600$ using HSE06 method) with a correlation coefficient of $R > 0.99$. By using this equation, it is possible to accurately control the band gap of the 1D extended graphdiyne nanowires by tuning the strength of the electric field.

Electronic properties with chemical functionalization

Scheme 2 shows eight models of the extended graphdiyne nanowires with chemically functionalized polyphenylene edges. The functional groups in these models include three activating groups (OH, NH_2, and CH_3), four deactivating groups (F, CN, NO_2, and COOH), and a combination of both activating (CH_3) and deactivating (NO_2) groups. In this work, substitution of the H atoms occurs only at the R^1–R^4 positions (Scheme 2). This is because the atoms would be overly crowded and thus result in rippled edges[52] if all of the 12 hydrogen atoms at the edges of the polyphenylene rings were substituted by functional groups. The obtained electronic band structures with the various substituents are shown in Figure 4.

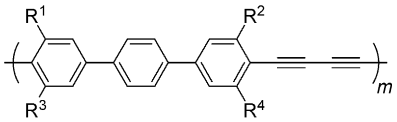

R^1, R^2, R^3, R^4 = OH
R^1, R^2, R^3, R^4 = NH_2
R^1, R^2, R^3, R^4 = CH_3
R^1, R^2, R^3, R^4 = F
R^1, R^2, R^3, R^4 = CN
R^1, R^2, R^3, R^4 = NO_2
R^1, R^2, R^3, R^4 = COOH
R^1, R^2 = CH_3; R^3, R^4 = NO_2

Scheme 2. The 1D extended graphdiyne nanowire with chemical functionalization.

Figure 4 shows that the extended graphdiyne nanowires with either activating or deactivating functional groups are still semiconductors with direct band gaps. This is quite similar to the trends observed in GNRs with varying functional groups.[52] Thus, the 1D extended graphdiyne nanowire could maintain its semiconducting property even with various functional group substitutions. Table 1 shows that the obtained band gaps of the substituted extended graphdiyne nanowires have a range of 1.023–1.708 eV using the PBE method (1.961–2.374 eV using HSE06 method). These band gap values are all smaller than the value of 1.762 eV (2.605 eV with HSE06) for pristine extended graphdiyne nanowire. It is also found that there is a decline in the energy levels of both the HOB and the LUB for the deactivating groups (F, CN, NO_2, and COOH), and an increase in the energy levels for the activating groups (OH, NH_2 and CH_3).

Because these extended nanowires are considered to be good candidates for nano-scaled electronics, an understanding of the charge carrier transport property would be advantageous. We studied the charge carrier mobility of the extended graphdiyne nanowires with varying functional groups based on a theoretical model using a deformation potential (DP) theory and an effective mass approach.[63,64] This model has been used for various carbon nanostructures such as fullerene chains, CNTs, and GNRs.[56,65,66] The charge carrier mobility μ of a 1D crystal can be expressed as:

$$\mu = \mathrm{e}\frac{\bar{\tau}}{|m^*|} \quad (1)$$

where m^* is the effective mass of charge carriers, and can be obtained by fitting the band structures;

$$m^* = \hbar^2 \left|\frac{\partial^2 E}{\partial k^2}\right|^{-1} \quad (2)$$

$\bar{\tau}$ is the average scattering relaxation time of the charge carrier. With the DP approximation, $\bar{\tau}$ of the 1D system is:

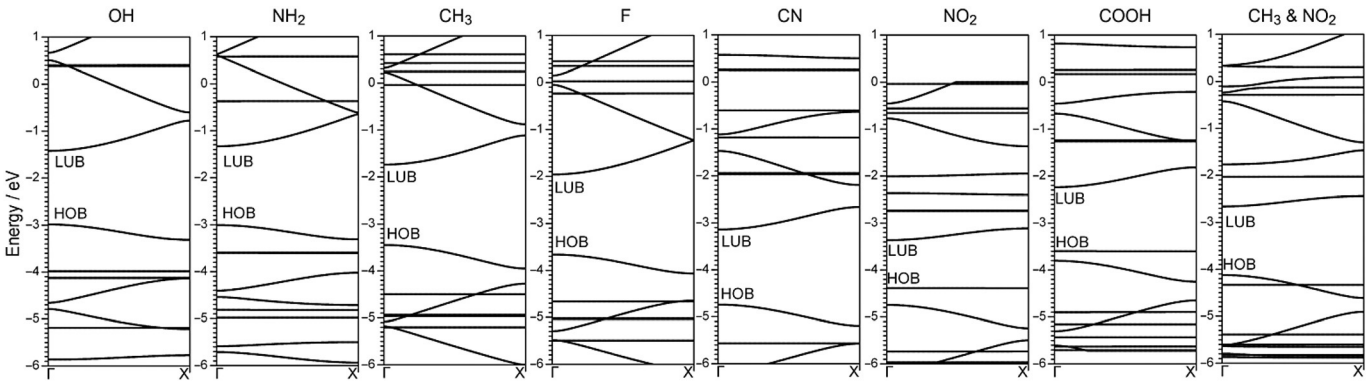

Figure 4. Band structures of the 1D extended graphdiyne nanowire with group substitutions as indicated at top.

Table 1. Electronic property and carrier mobility of the extended graphdiyne nanowires with group substitutions.[a]

Functional Group	HOB	LUB	E_g	E_g HSE06	C	E_{1v}	E_{1c}	m_h*	m_e*	μ_h	μ_e
OH	−2.987	−1.425	1.562	2.221	97.8	5.929	0.700	0.140	0.113	4.221×10^2	4.195×10^4
NH_2	−3.009	−1.335	1.674	2.344	105.9	6.120	1.138	0.115	0.120	5.743×10^2	1.556×10^4
CH_3	−3.450	−1.741	1.708	2.365	100.6	7.179	0.970	0.101	0.113	4.815×10^2	2.240×10^4
F	−3.664	−1.964	1.700	2.374	95.2	6.065	0.435	0.130	0.126	4.390×10^2	8.910×10^4
CN	−4.745	−3.143	1.602	2.233	95.5	4.946	0.697	0.101	0.127	9.714×10^2	3.445×10^4
NO_2	−4.389	−3.366	1.023	1.961	126.3	1.341	1.803	>10	0.153	/	5.160×10^3
COOH	−3.601	−2.243	1.358	2.178	129.2	0.190	1.291	>10	0.136	/	1.230×10^4
CH_3 & NO_2	−4.125	−2.664	1.461	2.080	112.1	6.549	2.559	0.123	0.183	4.796×10^2	1.742×10^3
pristine	−3.510	−1.750	1.760	2.605	94.6	6.600	0.340	0.136	0.117	3.547×10^2	1.500×10^5

[a] Units: HOB, LUB, E_g, E_{1v}, and E_{1c} in eV; C in eV Å^{-1}; m_h and m_h in m_e^0; μ_h and μ_e in cm^{2}V^{-1}s^{-1}.

$$\bar{\tau} = \frac{\hbar^2 C}{(2\pi|m^*|k_B T)^{1/2} E_1^2} \quad (3)$$

where C is the stretching modulus of a 1D crystal and can be obtained by:

$$C = L_0 \frac{\partial^2 E}{\partial L^2}\Big|_{L=L_0} \quad (4)$$

where L (L_0) is the lattice constant (equilibrium lattice constant). E_1 (including E_{1c} and E_{1v}) are DP constants for charge carriers (electron and hole) and can be obtained by:

$$E_1 = \left|\frac{L_0 \delta\varepsilon}{\delta L}\right| \quad (5)$$

Detailed descriptions can be referenced from our previous studies.[53,63] Notably, only longitudinal acoustic (LA) phonon scattering is considered in the models adopted here. Other scattering mechanisms such as optical phonon scattering, inter-sub-band scattering and radial-breathing phonon scattering that can also limit the charge mobility, are not addressed in this work. The LA phonon scattering is the main scattering mechanism due to its high coupling strength even at room temperature according to previous studies.[63,64,67,68] At low temperatures the optical phonon scattering is suppressed, and the electron scattering time by optical phonon remains almost unchanged with temperature due to the few excitation events.[68]

The calculated electron and hole mobilities for the extended nanowires at room temperature (T = 298 K) are listed in Table 1. The electron and hole mobilities (μ_e and μ_h) of the fabricated extended graphdiyne nanowire were calculated to be 1.500×10^5 and 3.547×10^2 cm^{2}V^{-1}s^{-1}, respectively. This electron mobility is three orders of magnitude larger than the hole. Thus, the transport of electrons in the extended graphdiyne nanowire is more favorable than the transport of holes. The m* value of the hole and the electron are very similar, although m_h* is slightly larger than m_e*. Therefore, the substantially larger electron mobility is mainly due to a smaller electron DP constant. The DP constants, E_{1v} and E_{1c}, are related to the band-edge shift induced by the scattering of the acoustic phonon at the HOCO and LUCO, respectively. As mentioned above, both the HOCO and LUCO delocalize in a longitudinal direction within the section of the carbon chain (Figure 2). Like the polyphenylene fragment, the HOCO spreads vertically in the longitudinal direction, but the LUCO is still oriented along the longitudinal direction. Thus the scattering by acoustic phonon for the HOCO is stronger than the LUCO, which leads to a larger E_{1v} value than the E_{1c} value for the extended wire. Therefore, the electron has a greater mobility than the hole for the extended graphdiyne nanowire.

We now focus on the chemical functionalization of the extended graphdiyne nanowire. It was found that the charge carrier mobilities of the extended graphdiyne nanowires with NO_2 and COOH groups exhibit rather distinctive properties relative to pristine and other chemically functionalized nanowires. Although there is a decrease in the E_{1V} values in comparison with pristine wire, the hole mobility of these two structures is rather low and close to zero. This can be attributed to the extremely large effective mass (>10 m_e) for the hole carrier, which is attributed to their rather flat HO bands (<0.005 eV). In the band structures, it is clear that the original HO-2 band (Figure 1a) shifts upward and becomes the HO band when the NO_2 and COOH groups are added to the extended graphdiyne nanowire. This is also confirmed by our crystal orbital studies. Figure 5 shows the HOCO and LUCO of the 1D nanowire with the NO_2 group. It is observed that the HOCO in NO_2-substituted nanowire is actually derived from the HO-2 orbital of the pristine nanowire. Furthermore, the HOCO in the NO_2-substituted nanowire exhibits clear localized characteristics, and is remarkably different from the delocalized features of the original HOCO of pristine nanowire. This fact explains the rather flat electronic energy band and the extremely large effective mass for the hole carrier of the NO_2-substituted nanowire. The electron mobilities are 5.16×10^3 and 1.23×10^4 cm^{2}V^{-1}s^{-1} for the NO_2 and COOH substituted models, respectively, which are one or two orders of magnitude smaller than the pristine wire. Because the stretching modulus and the effective mass are similar to the extended graphdiyne nanowire, the decreased electron mobility is mainly due to the larger DP constants for the two structures. The obtained DP constants for the electrons are 3.8- and 5.3-fold larger than the original nanowire if the NO_2 and COOH groups are added. A comparison of the LUCO of the extended graphdiyne nanowire before and after the NO_2 group is added is shown in Figures 2 and 5. Aside from the orbital distributions along the longitudinal direction, new branches that are oriented vertically relative to the longitudinal direction are also present in the added substituents. Thus, the scattering through acoustic phonon for the LUCO is stronger in the NO_2-substituted nanowire, which leads to a larger DP

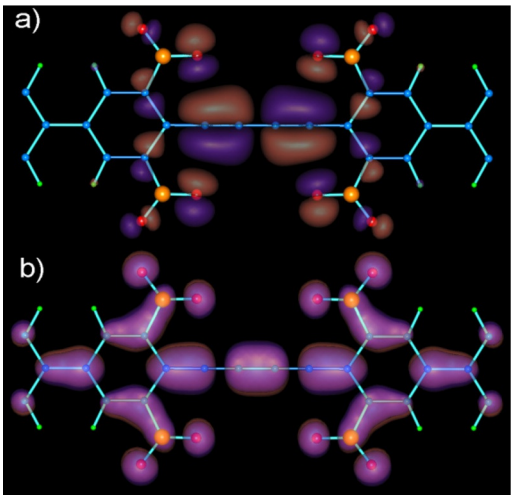

Figure 5. a) HOCO and b) LUCO of the NO_2-functionalized extended graphdiyne nanowire.

constant. Therefore, the electron mobility is always decreased with the addition of group substituents.

In the extended graphdiyne nanowires with F, CN, OH, NH_2, and CH_3 groups, it is found that the hole mobility still exhibits the same order as the pristine nanowire. This is because the stretching modulus, effective mass, and DP constants are all similar to those of the nanowire without any functional group substituents. The electron mobility is decreased by one order of magnitude relative to pristine wire if these groups are added. The reasoning for this observation is similar to our previously mentioned explanation of vertical orbital distributions in the LUCO for the substituted extended graphdiyne nanowires. Furthermore, the electron mobility is greater than the hole for each of the nanowires regardless of the presence of substituents on the nanowires.

Band gap and carrier mobility with carbon chain elongation

The synthesized extended graphdiyne nanowire can be seen as a junction with –C≡C– and polyphenylene as building blocks. Thus, the carbo-merized[23] graphdiyne nanowires, CGNW-*N* (Scheme 3) are built through an extension of the –C≡C– unit in the carbon chain portion. *N* denotes the number of –C≡C– units between the two fragments of polyphenylene. In this work, we decided to vary the number *N* from 2 to 20 in order to study the band gap and mobility of the extended graphdiyne nanowire upon carbo-merization. As shown in Figure S2 (Supporting Information), the obtained bond lengths of CGNW-*N* with *N* = 18–20 for the long and short C–C bonds in the center of the carbon chain fragment are 1.303 and 1.263 Å, respectively.

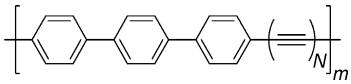

Scheme 3. Model of the carbo-merized extended graphdiyne nanowires.

Molecular dynamics (MD) simulations were also performed to further investigate the kinetic stability of the nanowires using the density-functional-based tight-binding (DFTB) method.[69] We performed three MD simulations for each structure at 300, 800, and 1200 K for 3 ps under constant-temperature and constant-volume conditions with the time step size set at 1 fs. CGNW-*N* with *N* = 5, 10, 15, and 20 are used as examples. The structures obtained after the MD calculations and the potential energies with time evolution are presented in Figure S3 (Supporting Information). We found that these 1D nanowires exhibit a moderate structural deformation under dynamic evolution, which was particularly true for the structures with long chains at high temperature. However, they remain very stable even at 1200 K after 3 ps of MD simulation. According to the MD simulations, these carbo-merized extended graphdiyne nanowires should be stable structures.

Figure 6 shows the calculated band structures of CGNW-*N* with *N* = 3, 5, 8, 9, 10, 15, and 20. Based on the band structures, it is clear that these extended nanowires have a direct band gap. Therefore, it can be concluded that the 1D carbo-merized nanowires are all semiconductors with direct band gaps. These results suggest that the semiconducting property of these 1D wires is independent of the –C≡C– chain sizes.

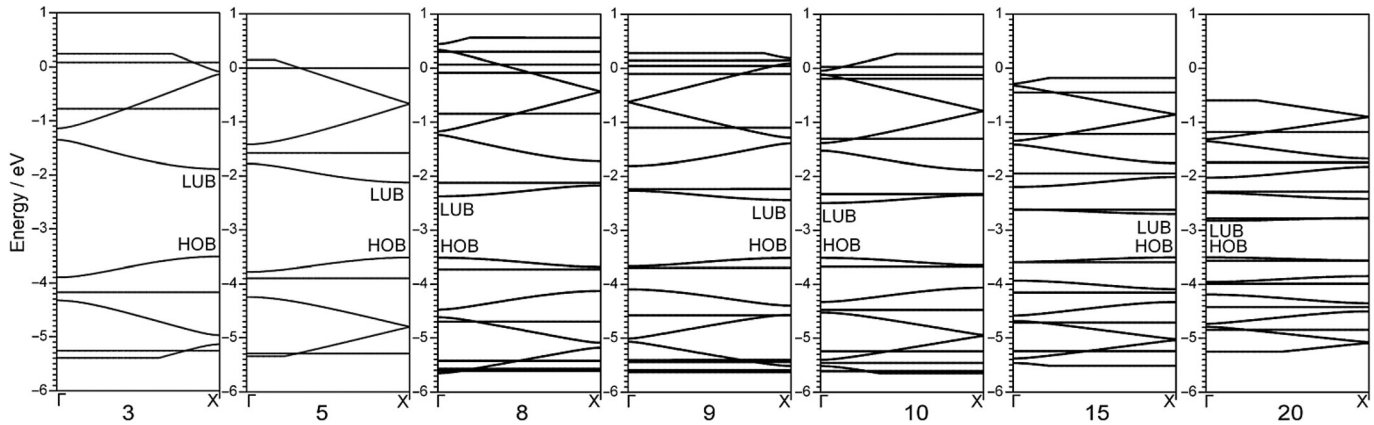

Figure 6. Electronic band structures of CGNW-*N* with *N* = 3, 5, 8, 9, 10, 15, and 20 as indicated at bottom.

Besides, the direct band gaps for the nanowires CGNW-*N* with $N=3$, 5, 9, 15 are all present at the X point in the first Brillouin zone, whereas they are at the Γ point for $N=8$, 10, and 20 according to the band structures shown in Figure 6. This is a very interesting phenomenon, as for all the carbo-merized nanowires tested, CGNW-*N* with *N* being even or odd always presented band gaps at the Γ or X points, respectively, in the first Brillouin zone. Thus it seems that the location of band gaps of these carbo-merized nanowires is determined only by the number of –C≡C– units.

The obtained band gaps of the carbo-merized nanowires are shown in Figure 7, and are calculated to fall within the range of 0.679–1.762 eV using the PBE method. These flexible band gaps open up the possibility of modulating the electronic properties of these 1D extended nanowires by tuning the sizes of the atomic carbon chains. Furthermore, it is observed that elongation of the carbon chain correlates to a decrease in the band gap, which means that a greater number of –C≡C– units would reduce the band gaps for the carbo-merized nanowires. The band gap of atomic carbon chain with BLA is only 0.228 eV, which is significantly smaller than 2.111 eV for 1D polyphenylene as mentioned above. Because these 1D extended nanowires are viewed as a junction with building blocks consisting of polyphenylene and carbon chain, this offers an explanation as to why the 1D wire with a greater number of –C≡C– units exhibits a smaller band gap. To obtain quantitative information on the relationship of the band gap to the composition of the extended nanowires, we plotted the E_g value of CGNW-*N* with respect to *N* in Figure 7. The band gaps of the 1D wires are fitted to the equation $E_g=0.537+1.542\times\exp(-N/8.549)$, for PBE calculations and $E_g=1.338+1.593\times\exp(-N/8.892)$ for HSE06 calculations with a correlation coefficient of $R>0.99$. This suggests that the band gaps of the hybrid nanowires will be primarily determined by the number of –C≡C– units. With these equations, it is possible to accurately control the band gaps by tuning the number of –C≡C– units in the 1D extended graphdiyne nanowires.

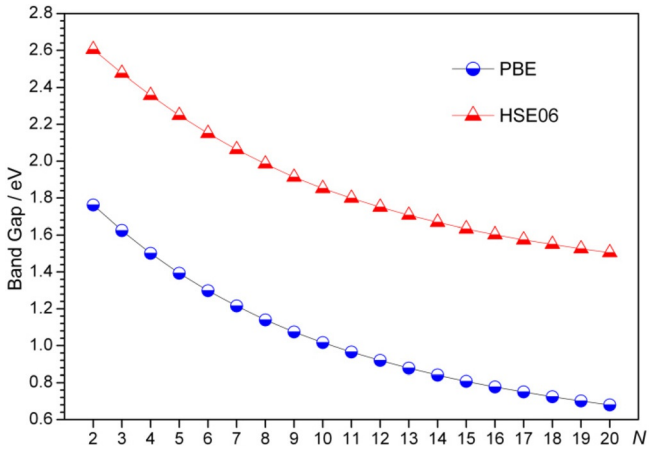

Figure 7. E_g with respect to the *N* value of CGNW-*N*.

The electron and hole mobilities were also calculated to further study the charge carrier transport properties of the extended nanowires. The calculated electron and hole mobilities for the extended nanowires at room temperature ($T=298$ K) are shown in Figure 8. It is found that the electron and hole mobilities (μ_e and μ_h) are within the range of 2.319×10^3–1.500×10^5 $cm^2V^{-1}s^{-1}$ and 3.547×10^2–2.709×10^3 $cm^2V^{-1}s^{-1}$ for the electrons and the holes, respectively. The mobility of organic semiconductors is usually less than 100 $cm^2V^{-1}s^{-1}$,[67,70] which is lower than the values obtained for the extended wires. However, the mobility of charge carriers for the 1D carbo-merized nanowires does draw close to the charge carrier mobility values for semiconducting CNTs and GNRs.[56,65,66] Thus, the 1D carbo-merized nanowires presented herein may be better candidates for high-mobility materials than organic semiconductors. Moreover, the electrons still have a larger mobility than the holes for the nanowires with short carbon chains (CGNW-*N* with $N\leq7$). In contrast, the electron and hole mobilities are quite similar in carbo-merized graphdiyne nanowires with very long carbon chains (CGNW-*N* with $N\geq12$).

We observed that the hole mobility increases as the sizes of the carbon chains increase in the extended nanowires. For instance, the hole mobility is 3.547×10^2 $cm^2V^{-1}s^{-1}$ in CGNW-2, but enlarges to 2.709×10^3 $cm^2V^{-1}s^{-1}$ in CGNW-20. Thus, it seems that longer carbon chains are favorable for hole transport. The opposite is observed for the electron mobilities, which are decreased as the carbon chains become longer. For comparison, the charge carrier mobility of the carbon chain with BLA was also calculated. The obtained electron and hole

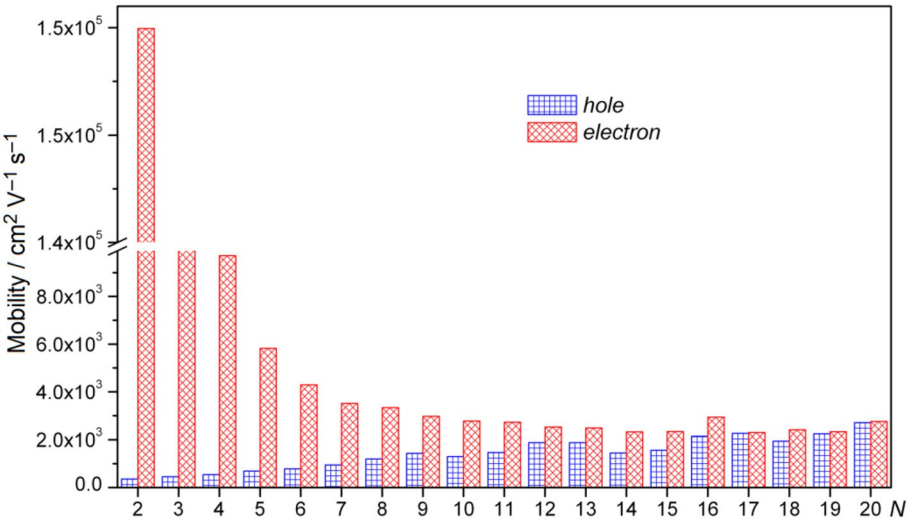

Figure 8. Charge carrier mobility of CGNW-*N*.

mobilities are 1.420×10^4 and 1.534×10^4 $cm^2V^{-1}s^{-1}$, respectively. Therefore, the carbo-merized graphdiyne nanowires with long carbon chains (CGNW-*N* with $N\geq5$) exhibit a smaller mobility by one or two orders of magnitude for both the electrons and holes than the pure carbon chain with BLA.

The obtained stretching modulus, the effective mass of charge carriers, and the DP constants for the 1D carbo-merized nanowires are listed in Table S2 (Supporting Information) in order to provide more insight into the charge mobility of the 1D nanowires. We first examine the stretching modulus, which exhibits an increasing trend within a range of 93–98 $eÅ^{-1}$, which falls between 90 $eÅ^{-1}$ for polyphenylene and 118 $eÅ^{-1}$ for the carbon chain. For the DP constants, the values of E_{1v} decrease, whereas the values of E_{1C} increase as the nanowires become longer. As a matter of fact, both the E_{1v} and E_{1c} values in CGNW-20 are substantially close to the values in atomic carbon chain with BLA. For the effective mass, it is found that the m^* value of both the hole and the electron decreases with elongation of the carbon chain. The obtained m_h^* and m_e^* values for CGNW-20 are 0.0785 and 0.0750 m_e^0, respectively. We are aware that the m^* for the carriers in CGNW-20 are still about twofold larger than the atomic carbon chain (0.0346 and 0.0327 m_e^0 for m_h^* and m_e^*). Because the stretching modulus and DP constants of CGNW-20 are similar to the atomic carbon chain, the decreased mobility of CGNW-20 is most likely derived substantially from the heavy carriers.

The frontier orbital of the atomic carbon chain is calculated in order to explain the change in the effective carrier masses for the carbo-merized graphdiyne nanowires. As shown in Figure S4 (Supporting Information), the HOCO and LUCO of the pure carbon chain exhibit perfect π-conjugation because all of the carbon atoms are exactly identical. Because the frontier orbital of the synthesized graphdiyne nanowire in Figure 2 can be seen as a combination of polyphenylene and a carbon chain, the π-conjugation system is therefore not as perfect as the carbon chain. Figure S5 (Supporting Information) shows that the π-system is well maintained along the extended wire axis in the carbo-merized graphdiyne nanowires. Additionally, the relative contribution to the frontier orbital from the atomic carbon chain greatly increases when the carbon chain is elongated. This leads to the fact that the frontier orbital of CGNW-*N* with a larger *N* tends to approach that of the pure carbon chain. As a result, the m^* values for both the hole and electron for CGNW-*N* also decrease and become closer to the pure carbon chain values as *N* is increased. Nevertheless, m^* is still larger than the carbon chain due to the presence of orbital derived from the polyphenylene part, although the longest extended nanowire in the studies included 20 $-C\equiv C-$ units.

Conclusions

On the basis of the first-principle DFT calculations, modulation of the electronic properties of the 1D extended graphdiyne nanowires was investigated by application of an electric field, chemical functionalization, and carbo-merization. Crystal orbital analysis was also performed to further ascertain the modulation of electronic properties.

When an electric field is applied in a direction perpendicular to the wire axis and parallel to the plane of the extended graphdiyne nanowire, the nanowire still exhibits semiconducting properties, with band gaps ranging from 1.762–2.000 eV. The relationship of the band gaps and the field strength was found to be $E_g=0.024E^2+1.760$, which would be useful for accurately controlling the band gap of the 1D extended graphdiyne nanowire based on the strength of the electric field.

The electronic properties of chemically functionalized 1D extended graphdiyne nanowires were also studied with several incorporated groups (OH, NH_2, CH_3, F, CN, NO_2, and COOH) at the polyphenylene edges. The functionalized extended graphdiyne nanowires with either activating or deactivating groups are still semiconductors despite the fact that the band gaps are somewhat smaller than those of pristine extended graphdiyne nanowire. The electron mobilities of the functionalized nanowires are one to two orders of magnitude smaller than those of pristine wire. The hole mobility of the extended graphdiyne nanowires with NO_2 and COOH groups is rather low and close to zero because of their rather flat HO bands.

The carbo-merized nanowires are built by elongation of the $-C\equiv C-$ unit in the carbon chain fragments of the extended graphdiyne nanowires. The extended nanowires exhibit decreasing band gaps in response to an elongating carbon chain. The band gap is fit to $E_g=0.537+1.542\times\exp(-N/8.549)$ in terms of the number of $-C\equiv C-$ units, which implies the possibility of tuning the band gaps by modifying the number of $-C\equiv C-$ units in the extended graphdiyne nanowire. The obtained electron and hole mobilities for the carbo-merized nanowires have values in the ranges of 2.319×10^3–1.500×10^5 $cm^2V^{-1}s^{-1}$ and 3.547×10^2–2.709×10^3 $cm^2V^{-1}s^{-1}$, respectively, which are clearly larger than the mobility values for organic semiconductors.

The modulation of band gap and carrier mobility of the extended graphdiyne nanowires influenced by several physical or chemical methods provides greater flexibility for energy band engineering as well as charge transport. These interesting findings indicate that the extended graphdiyne nanowire and its analogues are promising candidates for future applications in novel nanoelectronics and molecular devices. Thus, we believe that these results regarding graphdiyne-based materials will be helpful in moving these new fields forward.

Experimental Section

The energies, band structures, and properties of the extended graphdiyne nanowires in this work were computed with full structural optimizations using the SCF-CO method based on first-principle DFT calculations with the CRYSTAL09 program.[71,72] The exchange-correlation functional is addressed using the method proposed by Perdew, Burke, and Ernzerhof (PBE).[73] Because we are aware that the PBE functional would underestimate the band gaps of semiconductors, the band structures of the extended graphdiyne nanowires were also calculated using the more sophisticated hybrid functional method, HSE06. This method yields a more accurate approximation of the band gaps for carbon-based nanomaterials.[33] A double-ζ plus polarization basis set 6-21G(*d*,*p*) implemented in the program for solid-state calculations and an 80 *k*-points

sampling in the first Brillouin zone were adopted in the SCF-CO calculations. The default values for the convergence criteria in CRYSTAL09 were used in our calculations. In the calculations, we assume that all of the extended graphdiyne nanowires exhibit a coplanar conformation, which is a common treatment of π-conjugated systems.[43,74,75] It should be pointed out that the phenyl rings exhibit a flexible twist angle under different conditions.[76–82] The twist angles are ~30–40° in the gas phase, whereas in the bulk phase they adopt a more planar conformation, with inter-ring twist angles of ~10–20°.[76–78] Moreover, several studies have indicated that some oligomers of the poly(*para*-phenylene) adopt a planar configuration under high pressure, or on average with high librational amplitudes.[81,82] Actually, several conformations of the extended graphdiyne nanowire with twist angles in the range of 0–40° were also calculated with the same method for comparison. As shown in Figure S1 (Supporting Information), it was found that the obtained band structures of the conformations with different twist angles exhibit no qualitative difference, which agrees well with previous studies.[43]

Acknowledgements

This work is supported by the Natural Science Foundation of China (21363017 and 20873009).

Keywords: band gap engineering · carrier mobility · density functional theory · graphdiyne · nanomaterials

[1] A. Hirsch, *Nat. Mater.* **2010**, *9*, 868–871.
[2] C. K. Chua, M. Pumera, *Chem. Soc. Rev.* **2013**, *42*, 3222–3233.
[3] B. I. Kharisov, O. V. Kharissova, U. Ortiz-Mendez, *Handbook of Less-Common Nanostructures*, CRC Press, New York, **2012**, pp. 579–595.
[4] K. Refson, S. F. Parker, *ChemistryOpen* **2015**, *4*, 620–625.
[5] J. Li, H. Bai, N. Yuan, Y. Wu, Y. Ma, P. Xue, Y. Ji, *Int. J. Quantum Chem.* **2014**, *114*, 725–730.
[6] K. S. Novoselov, A. K. Geim, S. V. Morozov, D. Jiang, Y. Zhang, S. V. Dubonos, I. V. Grigorieva, A. A. Firsov, *Science* **2004**, *306*, 666–669.
[7] D. Jiang, Z. Chen, *Graphene Chemistry: Theoretical Perspectives*, John Wiley & Sons, New Delhi, **2013**, pp. 29–151.
[8] J. van der Lit, M. P. Boneschanscher, D. L. Vanmaekelbergh, M. Ijäs, A. Uppstu, M. Ervasti, A. Harju, P. Liljeroth, I. Swart, *Nat. Commun.* **2013**, *4*, 2023.
[9] E. Cunha, M. F. Proenca, F. Costa, A. J. Fernandes, M. A. C. Ferro, P. E. Lopes, M. González-Debs, M. Melle-Franco, F. L. Deepak, M. C. Paiva, *ChemistryOpen* **2015**, *4*, 115–119.
[10] R. Mazzaro, A. Boni, G. Valenti, M. Marcaccio, F. Paolucci, L. Ortolani, V. Morandi, P. Ceroni, G. Bergamini, *ChemistryOpen* **2015**, *4*, 268–273.
[11] R. J. Lagow, J. J. Kampa, H. Wei, S. L. Battle, J. W. Genge, D. A. Laude, C. J. Harper, R. Bau, R. C. Stevens, J. F. Haw, E. Munson, *Science* **1995**, *267*, 362–367.
[12] X. Guo, J. Zhang, J. Li, L. Jiang, J. Zhang, *Chem. Phys.* **2009**, *360*, 27–31.
[13] M. Weimer, W. Hieringer, F. Della Sala, A. Görling, *Chem. Phys.* **2005**, *309*, 77–87.
[14] M. Liu, V. I. Artyukhov, H. Lee, F. Xu, B. I. Yakobson, *ACS Nano* **2013**, *7*, 10075–10082.
[15] V. I. Artyukhov, M. Liu, B. I. Yakobson, *Nano Lett.* **2014**, *14*, 4224–4229.
[16] R. H. Baughman, *Science* **2006**, *312*, 1009–1110.
[17] X. Zhao, Y. Ando, Y. Liu, M. Jinno, T. Suzuki, *Phys. Rev. Lett.* **2003**, *90*, 187401.
[18] Y. Wang, Y. Huang, B. Yang, R. Liu, *Carbon* **2006**, *44*, 456–462.
[19] Y. Wang, Y. Huang, B. Yang, R. Liu, *Carbon* **2008**, *46*, 276–284.
[20] J. C. Meyer, C. O. Girit, M. F. Crommie, A. Zettl, *Nature* **2008**, *454*, 319–322.
[21] C. Jin, H. Lan, L. Peng, K. Suenaga, S. Iijima, *Phys. Rev. Lett.* **2009**, *102*, 205501.
[22] L. Shen, M. Zeng, S. Yang, C. Zhang, X. Wang, Y. Feng, *J. Am. Chem. Soc.* **2010**, *132*, 11481–11486.
[23] R. Chauvin, *Tetrahedron Lett.* **1995**, *36*, 397–400.
[24] C. Zou, C. Duhayon, V. Maraval, R. Chauvin, *Angew. Chem. Int. Ed.* **2007**, *46*, 4337–4341; *Angew. Chem.* **2007**, *119*, 4415–4419.
[25] P. Manini, W. Amrein, V. Gramlich, F. Diederich, *Angew. Chem. Int. Ed.* **2002**, *41*, 4339–4343; *Angew. Chem.* **2002**, *114*, 4515–4519.
[26] I. Hisaki, Y. Sakamoto, H. Shigemitsu, N. Tohnai, M. Miyata, S. Seki, A. Saeki, S. Tagawa, *Chem. Eur. J.* **2008**, *14*, 4178–4187.
[27] M. Iyoda, J. Yamakawa, M. J. Rahman, *Angew. Chem. Int. Ed.* **2011**, *50*, 10522–10553; *Angew. Chem.* **2011**, *123*, 10708–10740.
[28] V. Maraval, R. Chauvin, *Chem. Rev.* **2006**, *106*, 5317–5343.
[29] G. Li, Y. Li, H. Liu, Y. Guo, Y. Li, D. Zhu, *Chem. Commun.* **2010**, *46*, 3256–3258.
[30] J. Kang, J. Li, F. Wu, S. Li, J. Xia, *J. Phys. Chem. C* **2011**, *115*, 20466–20470.
[31] J. Chen, J. Xi, D. Wang, Z. Shuai, *J. Phys. Chem. Lett.* **2013**, *4*, 1443–1448.
[32] Y. Li, L. Xu, H. Liu, Y. Li, *Chem. Soc. Rev.* **2014**, *43*, 2572–2586.
[33] Q. Yue, S. Chang, J. Kang, S. Qin, J. Li, *J. Phys. Chem. C* **2013**, *117*, 14804–14811.
[34] V. Ongun Özçelik, S. Ciraci, *J. Phys. Chem. C* **2013**, *117*, 2175–2182.
[35] K. Srinivasu, S. K. Ghosh, *J. Phys. Chem. C* **2012**, *116*, 5951–5956.
[36] Z. Li, M. Smeu, A. Rives, V. Maraval, R. Chauvin, M. A. Ratner, E. Borguet, *Nat. Commun.* **2015**, *6*, 6321.
[37] Y. Ni, K. Yao, H. Fu, G. Gao, S. Zhu, B. Luo, S. Wang, R. Li, *Nanoscale* **2013**, *5*, 4468–4475.
[38] W. Wu, W. Guo, X. Zeng, *Nanoscale* **2013**, *5*, 9264–9276.
[39] W. Zhao, B. Cui, C. Fang, G. Ji, J. Zhao, X. Kong, D. Zou, X. Jiang, D. Li, D. Liu, *Phys. Chem. Chem. Phys.* **2015**, *17*, 3115–3122.
[40] X. Qian, Z. Ning, Y. Li, H. Liu, C. Ouyang, Q. Chen, Y. Li, *Dalton Trans.* **2012**, *41*, 730–733.
[41] G. Li, Y. Li, X. Qian, H. Liu, H. Lin, N. Chen, Y. Li, *J. Phys. Chem. C* **2011**, *115*, 2611–2615.
[42] J. Zhou, X. Gao, R. Liu, Z. Xie, J. Yang, S. Zhang, G. Zhang, H. Liu, Y. Li, J. Zhang, Z. Liu, *J. Am. Chem. Soc.* **2015**, *137*, 7596–7599.
[43] B. Cirera, Y. Zhang, J. Bjrk, S. Klyatskaya, Z. Chen, M. Ruben, J. V. Barth, F. Klappenberger, *Nano Lett.* **2014**, *14*, 1891–1897.
[44] E. Vergara, E. Arias, I. Moggio, C. Gallardo-Vega, R. F. Ziolo, R. M. Jiménez-Barrera, D. Navarro, O. Rodríguez, S. Fernández, M. Herrera, *Langmuir* **2015**, *31*, 6909–6916.
[45] J. Liu, Q. Chen, L. Xiao, J. Shang, X. Zhou, Y. Zhang, Y. Wang, X. Shao, J. Li, W. Chen, G. Q. Xu, H. Tang, D. Zhao, K. Wu, *ACS Nano* **2015**, *9*, 6305–6314.
[46] P. D. Jarowski, F. Diederich, K. N. Houk, *J. Org. Chem.* **2005**, *70*, 1671–1678.
[47] S. Roth, D. Carroll, *One-Dimensional Metals*, Wiley-VCH, Weinheim, **2004**, pp. 77–188.
[48] A. Facchetti, *Chem. Mater.* **2011**, *23*, 733–758.
[49] X. Guo, M. Baumgarten, K. Müllen, *Prog. Polym. Sci.* **2013**, *38*, 1832–1908.
[50] Y. Li, S. V. Rotkin, U. Ravaioli, *Nano Lett.* **2003**, *3*, 183–187.
[51] C. Chen, M. Lee, S. J. Clark, *Nanotechnology* **2004**, *15*, 1837–1843.
[52] G. Wang, H. Ge, *Chem. Phys.* **2014**, *439*, 57–62.
[53] H. Bai, Y. Zhu, W. Qiao, Y. Huang, *RSC Adv.* **2011**, *1*, 768–775.
[54] L. D. Pan, L. Z. Zhang, B. Q. Song, S. X. Du, H. J. Gao, *Appl. Phys. Lett.* **2011**, *98*, 173102.
[55] H. Bai, W. Qiao, Y. Zhu, Y. Huang, *Curr. Appl. Phys.* **2015**, *15*, 342–351.
[56] G. Wang, *Phys. Chem. Chem. Phys.* **2011**, *13*, 11939–11945.
[57] Y. Zhu, H. Bai, Y. Huang, *Synth. Met.* **2015**, *204*, 57–64.
[58] J. Ramirez, M. L. Mayo, S. Kilina, S. Tretiak, *Chem. Phys.* **2013**, *413*, 89–101.
[59] R. V. Salvatierra, G. Zitzer, S.-A. Savu, A. P. Alves, A. J. G. Zarbin, T. Chassé, M. B. Casu, M. L. M. Rocco, *Synth. Met.* **2015**, *203*, 16–21.
[60] J. Kang, F. Wu, J. Li, *J. Phys. Condens. Matter* **2012**, *24*, 165301.
[61] H. Raza, E. C. Kan, *Phys. Rev. B* **2008**, *77*, 245434.
[62] O. Cretu, A. R. Botello-Mendez, I. Janowska, C. Pham-Huu, J. C. Charlier, F. Banhart, *Nano Lett.* **2013**, *13*, 3487–3493.
[63] Y. Huang, R. Liu, *Chem. Res. Chin. Univ.* **1991**, *7*, 107–113.
[64] F. B. Beleznay, F. Bogar, J. Ladik, *J. Chem. Phys.* **2003**, *119*, 5690–5695.
[65] H. Bai, Y. Ai, Y. Huang, *Phys. Status Solidi B* **2011**, *248*, 969–973.

[66] W. Qiao, H. Bai, Y. Zhu, Y. Huang, *J. Phys. Condens. Matter* **2012**, *24*, 185302.
[67] J. Xi, M. Long, L. Tang, D. Wang, Z. Shuai, *Nanoscale* **2012**, *4*, 4348 – 4369.
[68] J. Xi, D. Wang, Z. Shuai, *WIREs Comput. Mol. Sci.* **2015**, *5*, 215 – 227.
[69] M. Elstner, D. Porezag, G. Jungnickel, J. Elsner, M. Haug, T. Frauenheim, S. Suhai, G. Seifert, *Phys. Rev. B* **1998**, *58*, 7260.
[70] L. Wang, G. Nan, X. Yang, Q. Peng, Q. Li, Z. Shuai, *Chem. Soc. Rev.* **2010**, *39*, 423 – 434.
[71] R. Dovesi, R. Orlando, B. Civalleri, C. Roetti, V. R. Saunders, C. M. Zicovich-Wilson, *Z. Kristallogr.* **2005**, *220*, 571.
[72] R. Dovesi, V. R. Saunders, C. Roetti, R. Orlando, C. M. Zicovich-Wilson, F. Pascale, B. Civalleri, K. Doll, N. M. Harrison, I. J. Bush, Ph. D'Arco, M. Llunell, *CRYSTAL09 User's Manual*, University of Torino, Torino (Italy), **2009**.
[73] J. P. Perdew, K. Burke, M. Ernzerhof, *Phys. Rev. Lett.* **1996**, *77*, 3865 – 3868.
[74] M. Kondo, D. Nozaki, M. Tachibana, T. Yumura, K. Yoshizawa, *Chem. Phys.* **2005**, *312*, 289 – 297.
[75] G. Koller, S. Berkebile, M. Oehzelt, P. Puschnig, C. Ambrosch-Draxl, F. P. Netzer, M. G. Ramsey, *Science* **2007**, *317*, 351 – 355.
[76] S. Müllegger, K. Hänel, T. Strunskus, C. Wöll, A. Winkler, *ChemPhysChem* **2006**, *7*, 2552 – 2558.
[77] H. Yanagi, T. Morikawa, *Appl. Phys. Lett.* **1999**, *75*, 187 – 189.
[78] N. Koch, G. Heimel, J. Wu, E. Zojer, R. L. Johnson, J. L. Brédas, K. Müllen, J. P. Rabe, *Chem. Phys. Lett.* **2005**, *413*, 390 – 395.
[79] F. Klappenberger, D. Kühne, M. Marschall, S. Neppl, W. Krenner, A. Nefedov, T. Strunskus, K. Fink, C. Wöll, S. Klyatskaya, O. Fuhr, M. Ruben, J. V. Barth, *Adv. Funct. Mater.* **2011**, *21*, 1631 – 1642.
[80] Y. Zhang, J. Björk, P. Weber, R. Hellwig, K. Diller, A. C. Papageorgiou, S. C. Oh, S. Fischer, F. Allegretti, S. Klyatskaya, M. Ruben, J. V. Barth, F. Klappenberger, *J. Phys. Chem. C* **2015**, *119*, 9669 – 9679.
[81] P. Puschnig, C. Ambrosch-Draxl, *Phys. Rev. B* **1999**, *60*, 7891 – 7898.
[82] S. Guha, W. Graupner, R. Resel, M. Chandrasekhar, H. R. Chandrasekhar, R. Glaser, G. Leising, *Phys. Rev. Lett.* **1999**, *82*, 3625.

Received: June 4, 2015
Published online on September 9, 2015

